DC Characteristics of InAlAs/InGaAsSb/InGaAs Double Heterojunction Bipolar Transistors

Shu-Han Chen, *Member, IEEE*, Chao-Min Chang, *Student Member, IEEE*, Pei-Yi Chiang, Sheng-Yu Wang, Wen-Hao Chang, and Jen-Inn Chyi, *Senior Member, IEEE*

***Abstract*—DC electrical characteristics of a series of InAlAs/InGaAsSb/InGaAs double heterojunction bipolar transistors (DHBTs) that are grown on InP by molecular beam epitaxy are reported and analyzed. The InGaAsSb base of the transistors leads to a type-I base–emitter junction and a type-II base–collector junction, resulting in unique device characteristics, such as low turn-on voltage, low crossover current, and constant current gain over a wide current range. In addition, the DHBTs exhibit rather high current gains despite the use of a heavily doped thick InGaAsSb base layer. This indicates the long minority carrier lifetime of the InGaAsSb material. A high current gain over base sheet resistance ratio is, thus, realized with these novel DHBTs.**

***Index Terms*—Heterojunction bipolar transistors (HBTs), InAlAs/InGaAsSb, type-II base–collector (B/C) junction.**

I. Introduction

RECENTLY, InP/GaAsSb/InP double heterojunction bipolar transistors (DHBTs) have been receiving increasing attention due to the staggered band alignment (type II) at their GaAsSb/InP base–collector (B/C) junction, which gives rise to higher collector current density and higher saturation velocity V_{sat} as compared with the conventional DHBTs [1]. Type-II GaAsSb/InP DHBTs with a high $f_T = 670$ GHz have been reported by using a graded GaAsSb/InGaAsSb base layer [2], [3]. On the other hand, the electron pileup effect, i.e., electron accumulation at the type-II InP/GaAsSb emitter–base (E/B) junction, often enhances the tunneling recombination current and affects current gain, particularly at low collector current levels [4]. This issue can be alleviated by transforming the E/B junction band alignment from type II to type I, for example, by using an InAlP or an InAlAs emitter for the GaAsSb base [4]–[6]. A composite InP/InGaP emitter has also been proposed for the same purpose. With a strained InGaP spacer and a graded GaAsSb base layer, impressive dc and microwave results are demonstrated in the InP/InGaP/GaAsSb/InP DHBT [7]. Although crystal quality of this material system still has room to improve, these reports suggest that eliminating the electron pileup effect at the type-II E/B junction is beneficial for high-performance InP-based DHBTs.

Previously, the authors proposed an InP/$\mathrm{In_{0.37}Ga_{0.63}As_{0.89}Sb_{0.11}/In_{0.53}Ga_{0.47}As}$ DHBT structure, which has type-I E/B and type-II B/C junctions, respectively [8], [9]. Low turn-on voltage, high current gain in the low-current regime, high collector current density, and high collector average electron velocity were simultaneously achieved for the InP/InGaAsSb/InGaAs DHBTs. Although the advantages of the aforementioned DHBTs are evident, the maximum frequency of oscillation $f_{\max}$ of the devices suffers from high base sheet resistance R_{SH}. This is due to the low p-type doping concentration and unoptimized growth condition of the InGaAsSb base layer. While increasing the doping concentration in the InGaAsSb base layer could decrease base sheet resistance, it might also decrease current gain due to the enhanced Auger process and/or impurity scattering. Interestingly, in an earlier study, Bolognesi *et al.* [10] reported on the suppressed Auger recombination in InP/GaAsSb DHBTs with a $\mathrm{p^+}$-GaAsSb base. The dc current gain of these DHBTs did not follow the quadratic reduction relation with increasing base doping concentration, indicating that the neutral base recombination is not governed by the Auger process but, rather, by hole confinement. Hence, low base sheet resistance can be achieved by increasing the doping concentration in a graded GaAsSb base while maintaining a reasonable current gain [7].

In this paper, a novel InGaAsSb base DHBT consisting of a type-I InAlAs/InGaAsSb E/B junction and a type-II InGaAsSb/InGaAs B/C junction is proposed. Fig. 1 illustrates the schematic band alignment of the proposed $\mathrm{In_{0.52}Al_{0.48}As}/\mathrm{In}_x\mathrm{Ga}_{1-x}As_{1-y}\mathrm{Sb}_y/\mathrm{In_{0.53}Ga_{0.47}As}$ DHBTs. Using an InAlAs emitter results in a type-I lineup, which avoids the electron pileup issue despite the high Sb content in the base that is used as compared with the type-II InP/$\mathrm{GaAs_{0.51}Sb_{0.49}}$ E/B junction. From the material growth aspect, the flux switching at the E/B interface becomes much simpler since no phosphorus compound is involved. In addition, the complicated spacer layer at the E/B junction is no longer necessary for transforming the type of the heterojunction. The turn-on voltage can also be reduced in this DHBT because both conduction band discontinuity of the InAlAs/InGaAsSb E/B junction and the band gap of the InGaAsSb base are decreased [11], [12]. Meanwhile,

Manuscript received April 8, 2010; revised July 10, 2010; accepted August 20, 2010. Date of publication September 30, 2010; date of current version November 19, 2010. This work was supported in part by the Ministry of Economic Affairs under Contract 94-EC-17-A-07-S1-0001 and in part by the National Science Council of Taiwan under Contract NSC-98-2221-E-008-099-MY3. The review of this paper was arranged by Editor S. Bandyopadhyay.

S.-H. Chen is with the Department of Electrical Engineering, National Central University, Jhongli 32001, Taiwan, and also with the Research Center for Applied Sciences, Academia Sinica, Taipei 11529, Taiwan.

C.-M. Chang, P.-Y. Chiang, and S.-Y. Wang are with the Department of Electrical Engineering, National Central University, Jhongli 32001, Taiwan.

W.-H. Chang is with the Department of Electrophysics, National Chiao Tung University, Hsinchu 300, Taiwan.

J.-I. Chyi is with the Department of Electrical Engineering and Department of Optics and Photonics, National Central University, Jhongli 32001, Taiwan, and also with the Research Center for Applied Sciences, Academia Sinica, Taipei 11529, Taiwan (e-mail: chyi@ee.ncu.edu.tw).

Color versions of one or more of the figures in this paper are available online at http://ieeexplore.ieee.org.

Digital Object Identifier 10.1109/TED.2010.2072927

0018-9383/$26.00 © 2010 IEEE

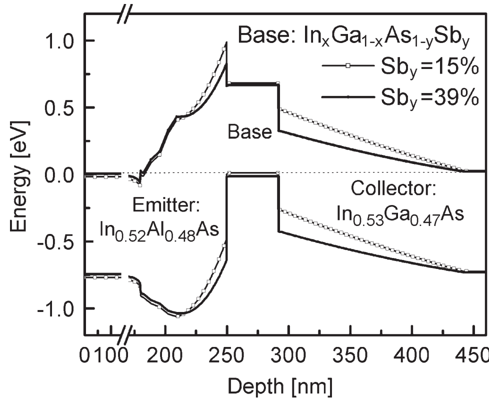

Fig. 1. Schematic band diagram of the InGaAsSb base DHBTs at zero bias.

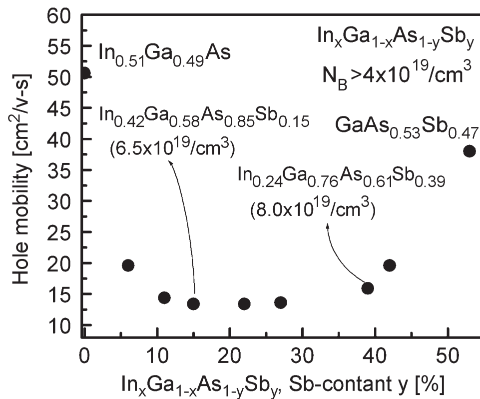

Fig. 2. Hole mobility of 66-nm-thick Be-doped InGaAsSb with different Sb contents.

the large valence band discontinuity at the InAlAs/InGaAsSb E/B junction prevents the back injection of holes from the base to the emitter, improving the electron injection efficiency. Consequently, low space charge recombination can also be expected in the abrupt InAlAs/InGaAsSb DHBTs.

The proposed type-II InGaAsSb/InGaAs B/C junction offers the advantages of high current density and high electron velocity [8]. The collector material can also be replaced by InP for high breakdown voltage consideration as long as the Sb content of the InGaAsSb layer is higher than 31% to maintain a type-II lineup [2].

II. Material Growth and Device Fabrication

The HBT epiwafers that are used in this study are grown on semiinsulating (100) InP substrates in a Riber 32P solid-source molecular beam epitaxy system (MBE) that is equipped with arsenic- and Sb-valved cracker cells. Since InGaAsSb is a material system that has not been well studied before, the basic properties of the system must be investigated. Several 66-nm-thick heavily Be-doped InGaAsSb samples crossing the entire composition range are grown. For the growth of a high Sb-content InGaAsSb layer that is lattice matched to InP, the Ga and In contents are adjusted to maintain a constant growth rate and V/III ratio. The hole mobility of these samples is characterized by room-temperature Hall measurements, as shown in Fig. 2. The hole mobility results show a U-shaped dependence on the Sb composition, implying the presence of a strong alloy-

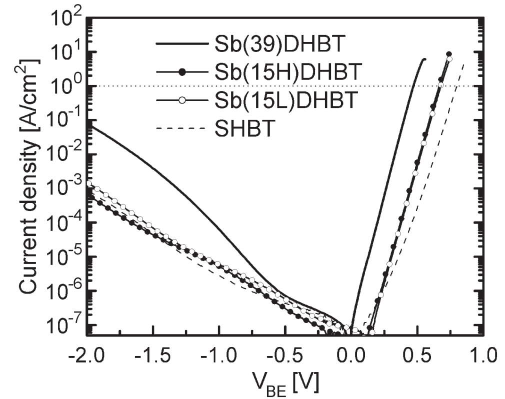

Fig. 3. E/B I–V characteristics of the InAlAs/InGaAsSb DHBTs and the conventional InAlAs/InGaAs SHBT.

scattering effect, which makes the hole mobility insensitive to the carrier concentration.

Three DHBT samples are prepared in this paper. They are designated as Sb(15H), Sb(15L), and Sb(39) and have a 44-nm-thick InGaAsSb base layer with Sb-content/doping concentration of $15\%/1.0 \times 10^{20}$ cm^{-3}, $15\%/6.5 \times 10^{19}$ cm^{-3}, and $39\%/1.1 \times 10^{20}$ cm^{-3}, respectively. As shown in Fig. 2, the hole mobility in InGaAsSb quaternary alloys is weakly dependent on the doping concentration. Different base-doping concentrations are used in Sb(15H) and Sb(15L) DHBTs to clarify the relation between the minority carrier (electron) lifetime and doping concentration, while different Sb composition in the InGaAsSb base layer is adopted to investigate the composition effects on carrier transport and current gain. A single heterojunction bipolar transistor (SHBT) with an InAlAs emitter and an InGaAs B/C junction is also prepared for comparison.

Large devices with an emitter size of 70×70 μm^2 are fabricated by the triple mesa wet-etching process. Pt/Ti/Pt/Au metal contacts are used for all the electrodes. The electrical characteristics of the devices are measured using an HP4156A semiconductor parameter analyzer.

III. Results and Discussion

A. I–V Characteristics

As illustrated in Fig. 1, both the conduction and valence bands move upward as the InGaAs base is replaced by the InGaAsSb base. The current-transport behavior of the InGaAsSb base DHBTs should accordingly change. Fig. 3 shows the E/B junction current–voltage (I–V) characteristics of the HBTs. The $V_{\rm BE}$ turn-on voltage of the Sb(15H,15L) and Sb(39) DHBTs decreases to 0.68 and 0.47 V, respectively, at a current density of 1 A/cm^2, whereas that of the conventional SHBT is 0.8 V. The decreased turn-on voltage is associated with a reduction of the base band gap and the conduction band offset as described in our previous study on InP/InGaAsSb/InGaAs DHBTs [8], [9], [11], [12]. The ideality factor of the InAlAs/InGaAsSb E/B junction is close to unity and is strong evidence of the reduced conduction band discontinuity when increasing the Sb content in the base.

As to the reverse characteristics, the breakdown behavior of the Sb(15H,15L) DHBTs is similar to that of the SHBT,

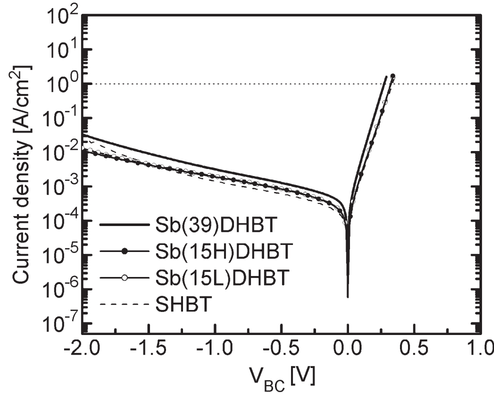

Fig. 4. B/C I–V characteristics of the InAlAs/InGaAsSb DHBTs and the conventional InAlAs/InGaAs SHBT.

indicating that adding 15% of Sb to the base layer has little effect on the E/B junction breakdown voltage. However, the breakdown voltage of the Sb(39) DHBT is obviously lower than that of the others. This could be due to the nonideal crystal growth of the $InAlAs/In_{0.24}Ga_{0.76}As_{0.61}Sb_{0.39}$ E/B junction.

Fig. 4 shows the B/C junction forward and reverse characteristics of the HBTs. In contrast to the E/B junction, the B/C junction characteristics of these HBTs are less dependent on the Sb content of the InGaAsSb base. Due to the absence of conduction band spike at the type-II B/C junction, the transport of carriers primarily follows the thermionic emission mechanism, and the turn-on voltage of the junction is basically related to the band gap of the InGaAsSb base. Through linear interpolation between the band gap of InAsSb and GaAsSb, the band gap of $In_{0.24}Ga_{0.76}As_{0.61}Sb_{0.39}$ is estimated to be 0.68 eV at 300 K [11], [13]. This is in good agreement with the 0.69 eV band-edge photoluminescence of a separate $In_{0.24}Ga_{0.76}As_{0.61}Sb_{0.39}$ bulk layer (not shown). This value is about 60–70 meV lower than that of the band gap of InGaAs (0.75 eV) at room temperature, which is consistently reflected by the reduced B/C junction turn-on voltage of the Sb(39) DHBT compared with the SHBT. As the band gap of $In_{0.42}Ga_{0.58}As_{0.85}Sb_{0.15}$ base layer is close to that of InGaAs, the B/C junction characteristics of the Sb(15H,15L) DHBTs and the SHBT are, thus, nearly identical, as shown in Fig. 4.

Due to the asymmetry of the I–V characteristics between the E/B and B/C junctions, the InGaAsSb base DHBTs with different common–emitter output characteristics are show in Fig. 5. The collector–emitter offset voltage $V_{\mathrm{CE,offset}}$ decreases from 470 mV for the conventional SHBT to 370 and 200 mV for the Sb(15H,15L) and Sb(39) DHBTs, respectively. Theoretically, the $V_{\mathrm{CE,offset}}$ can be calculated by [14]

$$V_{\mathrm{CE,offset}} = \frac{\eta_E kT}{q}\left(\frac{I_{\mathrm{CS}}}{\alpha_F I_{\mathrm{ES}}}\right) + \left(1 - \frac{\eta_E}{\eta_C}\right) \times (V_{\mathrm{BE}} - I_B R_B) + \frac{\eta_E}{\eta_C} I_B R_E \quad (1)$$

where η_C and η_E are the forward- and reverse-active ideality factors of the collector current and emitter current, respectively; α_F is the forward common–base current gain; I_{CS} and I_{ES} are the reverse saturation currents of E/B and B/C junctions; R_E and R_B are the emitter series resistance and base resistance, respectively. As indicated by the first term in (1), the offset voltage is partly contributed by $I_{\mathrm{CS}}/I_{\mathrm{ES}}$, which is, in turn, related to the symmetry of the E/B junction and B/C junction turn-on voltage. The second term in (1) describes the contribution of the forward- and reverse-active ideality factors, which result from the asymmetry of band alignment at the E/B and B/C junctions. The value of the last term is usually much smaller than that of the previous terms and can be neglected. As shown in Fig. 4, the turn-on voltage of the B/C junction is insensitive to the Sb content of the InGaAsSb base; the difference in $V_{\mathrm{CE,offset}}$ among these InGaAsSb DHBTs can thus be attributed to their different E/B junction turn-on voltage and forward-active ideality factor η_C that result from the different band alignment at the E/B junction of these InGaAsSb base DHBTs.

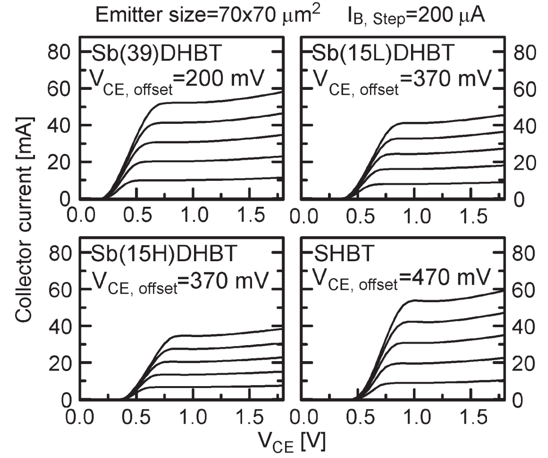

Fig. 5. Common–emitter output characteristics of the Sb(39) DHBT, Sb(15H,15L) DHBTs, and conventional SHBT.

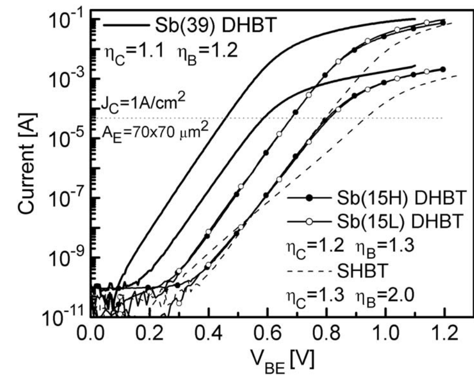

Fig. 6. Typical room-temperature Gummel plots for the InGaAsSb base DHBTs (solid line) and conventional SHBT (dashed line).

B. Gummel Plot and Current Gain

Fig. 6 shows the typical Gummel plots of the InGaAsSb base DHBTs and conventional SHBT. Clearly, the turn-on voltage of the Sb(39) DHBT is much lower than that of the SHBT. The ideality factor of the base current η_B is 1.2 and 1.3 for the Sb(39) DHBT and Sb(15H,15L) DHBTs, respectively, indicating that the bulk recombination current dominates over the space-charge recombination current $I_{B,\mathrm{scr}}$ compared with the η_B of 2.0 that is observed on the conventional SHBT. The

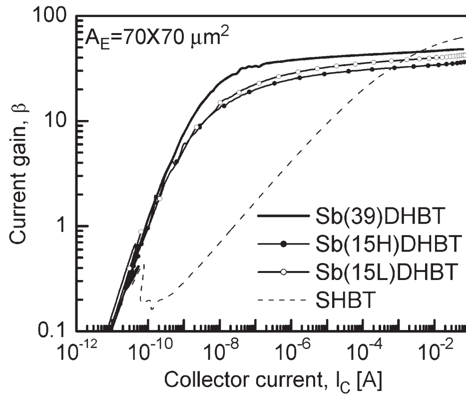

Fig. 7. Measured common–emitter current gain β as a function of collector current at $V_{\mathrm{CB}} = 0$ V.

low ideality factor maintains at low-current region, resulting in a lower crossover current of 1×10^{-10} A $(I_C = I_B, \beta = 1)$ compared with that of the conventional SHBT. Meanwhile, the current gain as a function of the collector current is plotted in Fig. 7. The InAlAs/InGaAsSb/InGaAs DHBTs maintain a reasonable current gain $(\beta > 20)$ for a wide collector current range from 4×10^{-8} to 8×10^{-2} A. At a collector current density J_C of 1 kA/cm^2 $(I_C = 49$ mA), the current gain of the Sb(39) DHBT is as high as 51 for a base-doping concentration of 1.1×10^{20} cm^{-3}. Another noteworthy characteristic of these devices is the weak dependence of their current gain on base doping N_B. The current gain is 35 and 44 for a base-doping concentration of 1.0×10^{20} cm^{-3} for the Sb(15H) DHBT and 6.5×10^{19} cm^{-3} for the Sb(15L) DHBT, showing the suppression of the neutral base recombination. This may be related to the intrinsic material property, such as the minority (electron) carrier lifetime.

C. Minority Carrier Lifetime in InGaAsSb DHBTs

To obtain more insight into the reason for the high current gain at such a high base doping level, the minority carrier (electron) lifetime τ_n of the Sb(15H,15L) DHBTs are estimated using the method that is reported by [10]. As discussed earlier, $I_{B,\mathrm{bulk}}$ dominates the total base current of the InGaAsSb DHBTs. The current gain of the DHBTs can, thus, be expressed as [14]

$$\beta = \frac{I_C}{I_{B,\mathrm{bulk}}} = \frac{\tau_n}{\tau_b} \tag{2}$$

where τ_n is the minority carrier (electron) lifetime in the base; τ_b is the base transit time in an uniformly doped base. In our previous work, the base-transit time of an $\mathrm{In_{0.37}Ga_{0.63}As_{0.89}Sb_{0.11}}$ base DHBT was estimated using an electron exit velocity V_{ext} of 2.54×10^7 cm/sec that is deduced from its current gain cutoff frequency. The electron diffusion coefficient D_n in the $\mathrm{In_{0.37}Ga_{0.63}As_{0.89}Sb_{0.11}}$ base was, thus, calculated to be 97 cm^2/sec (±10%) [8]. As the composition of the base is close to that of the Sb(15) DHBTs and D_n weakly depends on a p-type doping concentration ranging from 3.0×10^{19} cm^{-3} to 1.0×10^{20} cm^{-3} [15], the minority carrier lifetimes of the Sb(15) DHBTs are estimated using the same

TABLE I
ELECTRICAL PROPERTIES AND ESTIMATED MINORITY CARRIER LIFETIMES OF THE 44-nm-THICK $\mathrm{In_xGa_{1-x}As_{1-y}Sb_y}$ BASE DHBTs

HBT Sample	$\mathrm{Sb_y}$	$\mathrm{In_x}$	N_B ($\times 10^{19}$ cm^{-3})	β (1kA/cm^2)	τ_n (ps) Estimated	Rsh (Ohm/sq)	β/Rsh
Sb(15H)	15	42	10	35	9.5	1030	0.034
Sb(15L)	15	42	6.5	44	12.0	1743	0.025
Sb(39)	39	24	11	51	18.5	778	0.066
SHBT	0	53	4.2	62	-	663	0.093

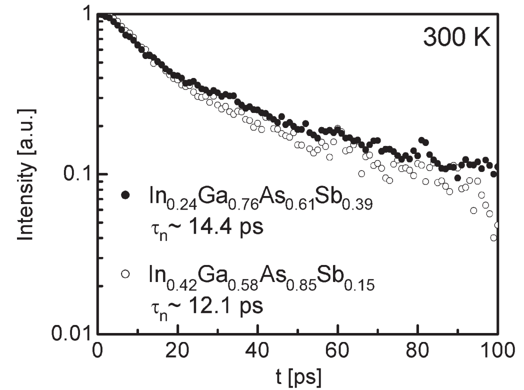

Fig. 8. Room-temperature time-resolved EC spectroscopy that is performed on $\mathrm{In_xGa_{1-x}As_{1-y}Sb_y}$ bulk samples. The lifetime/concentration for the $\mathrm{In_{0.24}Ga_{0.76}As_{0.61}Sb_{0.39}}$ and $\mathrm{In_{0.42}Ga_{0.58}As_{0.85}Sb_{0.15}}$ bulk layer is 14.4 ps/1.1×10^{20} cm^{-3} and 12.1 ps/6.5×10^{19} cm^{-3}, respectively.

D_n value. Since there is no report on D_n for InGaAsSb with a high Sb content, the D_n of Sb(39) DHBT is assumed to be 51 cm^2/sec (±30%). This value is arrived at through linear interpolation between the reported value of 43 cm^2/sec for $\mathrm{GaAs_{0.62}Sb_{0.38}}$ and 120 cm^2/sec for $\mathrm{In_{0.53}Ga_{0.47}As}$ [15]–[17]. The estimated minority carrier lifetime τ_n, along with the other parameters of the DHBTs, are summarized in Table I.

As shown in Table I, the minority carrier lifetimes τ_n are calculated to be 9.5 and 12.0 ps for the Sb(15H) and Sb(15L) DHBTs, respectively. The τ_n that is estimated here shows weak dependence on N_B, which is similar to that observed for InP/GaAsSb/InP DHBTs [10]. The calculated τ_n for the Sb(39) DHBT is 18.5 ps, which is longer than the τ_n for the Sb(15) DHBTs.

The minority carrier lifetimes are also checked on a separate set of InGaAsSb bulk layers by time-resolved excitation correlation (EC) spectroscopy, as shown in Fig. 8. The EC signal is extracted from the sum-frequency component by using a lock-in amplifier. The carrier lifetime can be determined by monitoring the EC signal as a function of the interpulse delay time γ. For the heavily doped InGaAsSb samples that are investigated here, the EC signal predominantly arises from the effect of differential absorption: the photocarriers that are generated by the first pulse make the second pulse less likely to excite as many photocarriers due to fewer available states. Therefore, the decay traces are governed by the minority carrier lifetime in the heavily doped background, as shown in Fig. 8.

TABLE II
MINORITY CARRIER LIFETIMES THAT ARE MEASURED BY TIME-RESOLVED EC SPECTROSCOPY FOR THE 66-nm-THICK $In_xGa_{1-x}As_{1-y}Sb_y$ BULK LAYERS

Bulk Sample	Sb_y	In_x	N_B ($\times 10^{19}$ cm^{-3})	τ_n (ps) measured	Rsh (Ohm/sq)
Sb(15)	15	42	6.5	12.1	1029
Sb(39)	39	24	11	14.4	521

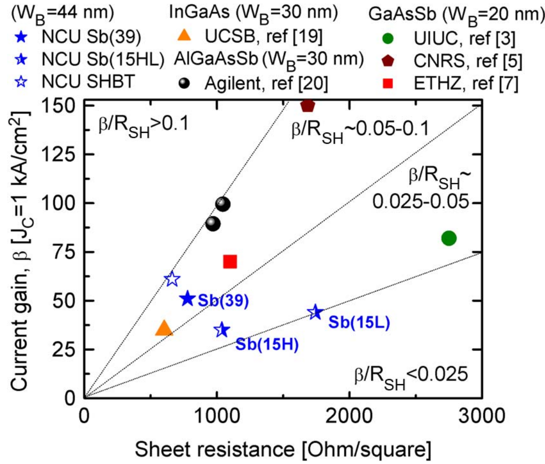

Fig. 9. Current gain β versus base sheet resistance R_{SH} for InGaAs, GaAsSb, and InGaAsSb base HBTs.

Table II lists the τ_n that are deduced for the 66-nm-thick InGaAsSb bulk layers. For the $In_{0.42}Ga_{0.58}As_{0.85}Sb_{0.15}$ sample, the deduced τ_n is 12.1 ps, which is in good agreement with the τ_n that is estimated for the Sb(15L) DHBT. However, there exists a discrepancy in the τ_n, which is 18.5 ps versus 14.4 ps, that are obtained by the two methods for $In_{0.24}Ga_{0.76}As_{0.61}Sb_{0.39}$. This could be due to an underestimation in the D_n of the Sb(39) DHBT. For a τ_n of 14.4 ps, the D_n has to be 90, which is close to that of the Sb(15L) DHBT. As the experimental results show, the D_n might also have a weak dependence on the Sb content, which is similar to the case of hole mobility that is depicted in Fig. 2. The observed long electron lifetime ($\tau_n > 10$ ps) in InGaAsSb is rather unique as compared with that of the $In_{0.53}Ga_{0.47}As$ and $GaAs_{0.51}Sb_{0.49}$ materials at similar doping concentrations. The possible reason for the longer τ_n in heavily Be-doped InGaAsSb could be the smaller Auger recombination coefficient in InGaAsSb [18].

The base sheet resistance R_{SH} of the InAlAs/InGaAsSb/InGaAs DHBTs that is characterized by the transfer length method is listed in Table I. Since both current gain and electron lifetime show weak dependence on base-doping concentration, while the base sheet resistance decreases with increasing doping concentration, a high β/R_{SH} value of 0.034 is observed for the Sb (15H) DHBT. Moreover, the Sb(39) DHBT exhibits a high current gain of 51 and a low base sheet resistance of 778 ohms per square, leading to an even higher β/R_{SH} value of 0.066. With similar base-doping level, the higher β/R_{SH} value for Sb(39) over Sb(15H) is attributed to the longer minority carrier lifetime and higher hole mobility of the $In_{0.24}Ga_{0.76}As_{0.61}Sb_{0.39}$ base. Fig. 9 shows the current gain versus the base sheet resistance for HBTs with an InGaAs, GaAsSb, or InGaAsSb base [3], [5], [7], [19], [20]. As shown in this figure, the Sb(39) DHBT has an excellent β/R_{SH} ratio and compares well to the state-of-the-art InP/InGaAs and InP/GaAsSb DHBTs.

IV. CONCLUSION

The dc electrical characteristics of the novel InAlAs/InGaAsSb/InGaAs DHBTs with different Sb contents have been systematically investigated. The V_{CE} offset and the turn-on voltages decrease with increasing Sb content, which is accounted for by the band lineups at the E/B and B/C junctions. The current gain of the DHBTs show weak dependence on the doping concentration, suggesting that low base sheet resistance can be achieved by increasing the doping concentration. The minority carrier lifetimes of InGaAsSb layers that have been measured by the time-resolved EC spectroscopy are longer than those of InGaAs and GaAsSb, supporting the high current gain that have been observed on these DHBTs despite their high base doping and thick base layer. A current gain/base sheet resistance ratio (β/R_{SH}) as high as 0.066 has been achieved on the DHBTs with an $In_{0.24}Ga_{0.76}As_{0.61}Sb_{0.39}$ base. These experimental results demonstrate the potential of the proposed DHBTs for low-power high-speed digital circuits.

REFERENCES

[1] C. R. Bolognesi, M. W. Dvorak, O. Pitts, S. P. Watkins, and T. W. MacElwee, "Investigation of high-current effects in staggered lineup InP/GaAsSb/InP heterostructure bipolar transistors: Temperature characterization and comparison to conventional type-I HBTs and DHBTs," in *IEDM Tech. Dig.*, 2001, pp. 768–771.

[2] W. Snodgrass, B. R. Wu, K. Y. Cheng, and M. Feng, "Type-II GaAsSb/InP DHBTs with record $f_T = 670$ GHz and simultaneous f_T, $f_{\mathrm{MAX}} >$ 400 GHz," in *IEDM Tech. Dig.*, 2007, pp. 663–666.

[3] W. Snodgrass and M. Feng, "Nano-scale Type-II InP/GaAsSb DHBTs to reach THz cutoff frequencies," in *Proc. GaAs MANTECH Conf.*, 2008, pp. 277–280.

[4] Y. Oda, H. Yokoyama, K. Kurishima, T. Kobayashi, N. Watanabe, and M. Uchida, "Improvement of current gain of C-doped GaAsSb-base heterojunction bipolar transistors by using an InAlP emitter," *Appl. Phys. Lett.*, vol. 87, no. 2, p. 023 503, Jul. 2005.

[5] M. Zaknoune, H. Colder, D. A. Yarekha, G. Dambrine, and F. Mollot, "Current gain enhancement in GaAsSb/InP—DHBT type grown by MBE with a graded composition AlInP emitter," in *Proc. IPRM*, May 2008, pp. 1–3.

[6] S. W. Cho, J. H. Yun, D. H. Jun, J. I. Song, I. Adesida, N. Pan, and J. H. Jang, "High performance InP/InAlAs/GaAsSb/InP double heterojunction bipolar transistors," *Solid State Electron.*, vol. 50, no. 6, pp. 902–907, Jun. 2006.

[7] H. G. Liu, O. Ostinelli, Y. Zeng, and C. R. Bolognesi, "600 GHz InP/GaAsSb/InP DHBTs grown by MOCVD with a Ga(As,Sb) graded-base and $f_T \times BV_{\mathrm{CEO}} > 2.5$ THz V at room temperature," in *IEDM Tech. Dig.*, 2007, pp. 667–670.

[8] S. H. Chen, K. H. Teng, H. Y. Chen, S. Y. Wang, and J.-I. Chyi, "Low turn-on voltage and high-current $InP/In_{0.37}Ga_{0.63}As_{0.89}Sb_{0.11}/In_{0.53}Ga_{0.47}As$ double heterojunction bipolar transistors," *IEEE Electron Device Lett.*, vol. 29, no. 7, pp. 655–657, Jul. 2008.

[9] S. H. Chen, H. Y. Chen, S. Y. Wang, K. H. Teng, and J.-I. Chyi, "Pseudomorphic InGaAsSb base DHBT grown by solid-source molecular beam epitaxy," in *Proc. 15th Int. Conf. Molecular Beam Epitaxy*, Vancouver, BC, Canada, Aug. 2008, p. 243.

[10] C. R. Bolognesi, H. G. Liu, N. Tao, X. Zhang, S. Bagheri-Najimi, and S. P. Watkins, "Neutral base recombination in InP/GaAsSb/InP double-heterostructure bipolar transistors: Suppression of Auger recombination

in p^+ GaAsSb base layers," *Appl. Phys. Lett.*, vol. 86, no. 25, p. 253 506, 2005.

[11] I. Vurgaftman, J. R. Meyer, and L. R. Ram-Mohan, "Band parameters for III–V compound semiconductors and their alloys," *J. Appl. Phys.*, vol. 89, no. 11, pp. 5815–5875, Jun. 2001.

[12] S. H. Chen, S. Y. Wang, R. J. Hsieh, and J.-I. Chyi, "InGaAsSb/InP double heterojunction bipolar transistors grown by solid-source molecular beam epitaxy," *IEEE Electron Device Lett.*, vol. 28, no. 8, pp. 679–681, Aug. 2007.

[13] M. Levinshtein, S. Rumyantsev, and M. Shur, *Hand Book Series on Semiconductor Parameters*. Singapore: World Scientific, 1996.

[14] W. Liu, *Handbook of III–V Heterojunction Bipolar Transistors*. New York: Wiley-Interscience, 1998.

[15] T. Kaneto, K. W. Kim, and M. A. Littlejohn, "A comparison of minority electron transport in $In_{0.53}Ga_{0.47}As$ and GaAs," *Appl. Phys. Lett.*, vol. 63, no. 1, pp. 48–50, Jul. 1993.

[16] H. G. Liu, N. Tao, S. P. Watkins, and C. R. Bolognesi, "Extraction of the average collector velocity in high-speed 'type-II' InP-GaAsSb-InP DHBTs," *IEEE Electron Device Lett.*, vol. 25, no. 12, pp. 769–771, Dec. 2004.

[17] G. Zohar, S. Cohen, V. Sidorov, A. Gavrilov, B. Sheinman, and D. Ritter, "Reduction of base-transit time of InP–GaInAs HBTs due to electron injection from an energy ramp and base-composition grading," *IEEE Trans. Electron Devices*, vol. 51, no. 5, pp. 658–662, May 2004.

[18] D. Vignaud, D. A. Yarekha, J. F. Lampin, M. Zaknoune, S. Godey, and F. Mollot, "Electron lifetime measurements of heavily C-doped InGaAs and GaAsSb as a function of the doping density," *Appl. Phys. Lett.*, vol. 90, no. 24, p. 242 104, Jun. 2007.

[19] Z. Griffith, E. Lind, and M. J. W. Rodwell, "Sub-300 nm InGaAs/InP type-I DHBTs with a 150 nm collector, 30 nm base demonstrating 755 GHz $f_{\max}$ and 416 GHz f_T," in *Proc. IPRM*, May 2007, pp. 403–406.

[20] B. R. Wu, W. Snodgrass, M. W. Dvorak, P. A. Colbus, T. S. Low, and D. D'Avanzo, "Performance improvement of composited-graded AlGaAsSb/InP double heterojunction bipolar transistors," in *Proc. IPRM*, May 2009, pp. 20–23.

Shu-Han Chen (M'03) was born in Hsinchu, Taiwan, on March 21, 1978. He received the B.S. and Ph.D. degrees in electrical engineering from the National Central University, Jhongli, Taiwan, in 2000, and 2008, respectively.

He is currently a Postdoctoral Fellow with the Research Center for Applied Science, Taipei, Taiwan. His current research interests include molecular beam epitaxial growth of Sb-based materials and related devices.

Chao-Min Chang (S'09) was born in Taichung, Taiwan, on November 27, 1984. He received the B.S. degree in electrical engineering from Dayeh University, Changhua, Taiwan, in 2007 and the M.S. degree in electrical engineering from the National Central University, Jhongli, Taiwan, in 2009, where he is currently working toward the Ph.D. degree in electric engineering.

His research has been focused on the molecular beam epitaxial growth of III–V heterojunction bipolar transistors.

Pei-Yi Chiang was born in Taipei, Taiwan, on June 5, 1985. She received the B.S. degree in electrical engineering from the National Changhua University of Education, Changhua, Taiwan, in 2007 and the M.S. degree in electrical engineering from the National Central University, Jhongli, Taiwan, in 2009.

Her research interests include the emitter size effect and the metal contact of Sb-based double heterojunction bipolar transistors.

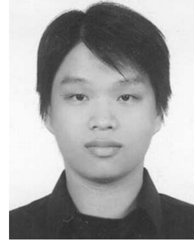

Sheng-Yu Wang was born in Tainan, Taiwan, on December 25, 1979. He received the B.S. and M.S. degrees in electrical engineering from the National Central University, Jhongli, Taiwan, in 2002, and 2004, respectively. He is currently working toward the Ph.D. degree in the electrical engineering at National Central University, Jhongli, Taiwan.

His research has been focused on electron-beam lithography for nanoscale heterojunction bipolar transistors.

Wen-Hao Chang received the B.S., M.S., and Ph.D. degrees in physics from the National Central University (NCU), Jhongli, Taiwan, in 1994, 1996, and 2001, respectively.

After spending four years as a Postdoctoral Researcher with the NCU, he joined the Department of Electrophysics, College of Science, National Chiao Tung University, Hsinchu, Taiwan, as an Assistant Professor and as an Associate Professor in 2005 and 2009, respectively. His research interests include the optical properties of low-dimensional semiconductor nanostructures and their applications in quantum optics, including the generation of single photons and entangled photon pairs, spin dynamics in quantum dots, and the magnetooptical properties of semiconductor nanostructures.

Jen-Inn Chyi (M'94–SM'98) received the B.S. and M.S. degrees in electrical engineering from the National Tsing-Hua University, Hsinchu, Taiwan, in 1982 and 1984, respectively, and the Ph.D. degree in electrical engineering from the University of Illinois, Urbana-Champaign, in 1990. His Ph.D. dissertation dealt with molecular beam epitaxial (MBE) growth and characterization of InSb on GaAs.

In 1991, he joined the Department of Electrical Engineering, National Central University (NCU), Jhongli, Taiwan. Since then, he has established MBE, metal–organic vapor phase epitaxy (MOVPE), and high-speed optoelectronic devices laboratories, which house growth and characterization facilities for various III–V materials and devices. He was the Director of the Optical Sciences Center, NCU, from 2000 to 2007. He is currently the Dean of the College of Electrical Engineering and Computer Science and the Chair Professor of Electrical Engineering, NCU. His research interests include the areas of MBE and MOVPE growth of III–V semiconductors and their heterostructures for high-speed electronic and optoelectronic devices. He has authored or coauthored over 260 journal papers and is the holder of 22 patents. His current research projects include MBE growth of InP-based heterojunction bipolar transistors, quantum dot photonic devices, MOVPE growth of GaN-based materials for ultraviolet, blue, and green emitters, and high-temperature high-power devices.

Dr. Chyi is a member of the Phi Tau Phi. He was the recipient of the 1996 Distinguished Young Researcher Award from the Electronic Devices and Materials Association and the 2002 and 2010 Distinguished Research Award from the National Science Council. He was the recipient of the Distinguished Professor Award from the Chinese Institute of Electrical Engineering and the Industrial Technology Advancement Award from the Ministry of Economic Affairs in 2004 and 2008, respectively. He has also served as a Distinguished Lecturer of the IEEE Electron Devices Society since 2004. He is an Associate Editor with the *IEEE Photonics Technology Letters* and the *Japanese Journal of Applied Physics*.